Effect of chloride introduction on the optical properties in Eu^{3+}-doped fluorozirconate glasses*

Han Jin(金含), Zhao-Jun Mo(莫兆军)†, Xiao-Song Zhang(张晓松), Lin-Lin Yuan(苑琳琳), Ming Yan(晏明), and Lan Li(李岚)‡

Institute of Material Physics, Key Laboratory for Optoelectronic Materials and Devices of Tianjin, Key Laboratory of Display Materials and Photoelectric Devices of Ministry of Education, Tianjin University of Technology, Tianjin 300384, *China*

(Received 4 February 2016; revised manuscript received 23 May 2016; published online 25 August 2016)

Fluorozirconate glass containing Eu^{3+} ions and chloride ions are prepared by a meltquenching method. The luminescence behavior of Eu^{3+} affected by Cl ions is investigated. With increasing Cl ion concentration, the luminous intensity of Eu^{3+} is significantly enhanced and the quantum efficiency of fluorozirconate glass is improved. Meanwhile, the intensity parameter Ω_2 increases according to the Judd–Ofelt calculation, which indicates the decrease of local symmetry. The average lifetime of Eu^{3+} increases by introducing the Cl ions. Moreover, we find two kinds of sites for Eu^{3+} ions in a glass network by analyzing the fluorescence decay. The distribution of Eu^{3+} ions changes with increasing Cl ion concentration. In addition, the excessive Cl ions lead to the separation of the glass phase and the formation of the crystal phase, thus reducing the transmittance dramatically.

Keywords: photoluminescence, fluorescence decay, Judd–Ofelt theory, quantum efficiency

PACS: 32.50.+d, 66.30.hh **DOI:** 10.1088/1674-1056/25/10/103201

1. Introduction

Rare-earth-doped glasses are known to be good candidate materials for devices such as optical fiber amplifiers, the solar cell conversion layers, solid state lasers, and so on.[1–5] Among these glasses, the fluorozirconate (FZ) glass has the most efficient luminescence that originates from the following characteristics: high transmittance from the visible to middle infrared region, low phonon energy, and higher solubility of rare earth ions.[6–8]

The substitution of chloride or bromide for fluorine in fluorozirconate glass around the rare earth ion changes the glass properties because the difference in ligand field symmetry between F–Cl and F–Br mixed-anion glasses. The presence of chloride or bromide helps to improve fluorescence emission efficiency because the phonon energies of chlorides and bromides are smaller than those of fluorides.[9] The transformation of fluorochlorozirconate (FCZ) and fluorobromozirconate (FBZ) glasses to glass-ceramics can obviously improve the spectroscopic properties of the material and other properties.[10]

Chloride or mixed halide glasses have a better transmission range due to the higher fundamental vibration frequency of the glass network.[11] Soga *et al.*[12] calculated the crystal field parameters of FCZ glass by a molecular dynamic simulation and point charge model of the crystal field; the results further showed that chlorine ions tended to coordinate to Eu^{3+} ion in zirconium rich glass and affected the luminescence properties of Eu^{3+} ions. Photoluminesence in Eu-doped fluorozirconate glass ceramic arises from Eu^{2+} ions in those $BaBr_2$ crystals, which has potential applications as x-ray storage phosphor.[13]

Fluorescence spectra and Judd–Ofelt (JO) theory provide useful information for characterizing luminescence properties and coordination environments around active rare earth ion in glasses. In this paper, we chose the Eu^{3+} ion as the probe to discuss the luminescence behavior of fluorozirconate glass doped with Cl ions due to its different sensitivities to the ligand field between the magnetic dipole transition $^5D_0 \rightarrow {}^7F_1$ and electric dipole transition $^5D_0 \rightarrow {}^7F_2$. Due to the energy gap between $^5D_0$ and the next lower level being more than 1.2×10^4 cm^{-1}, luminescence properties of Eu^{3+} would hardly be affected by the phonon energy of the matrix. The influences on the structure and characteristic temperature parameters of FZ glass affected by Cl ions are analyzed by the differential thermal analysis (DTA) and the x-ray diffraction (XRD). We obtain the correlation among luminescence intensity, lifetime, and the ligand field symmetry through the fluorescence spectra, the fluorescence decay, and the Judd–Ofelt parameters.

*Project supported by the National High Technology Research and Development Program of China (Grant No. 2013AA014201), the Natural Science Foundation of Tianjin, China (Grant Nos. 14JCZDJC31200, 15JCYBJC16700, and 15JCYBJC16800), the National Key Foundation for Exploring Scientific Instrument of China (Grant No. 2014YQ120351), and the International Cooperation Program from Science and Technology of Tianjin, China (Grant No. 14RCGHGX00872).

†Corresponding author. E-mail: mzjmzj163@163.com

‡Corresponding author. E-mail: lilan@tjut.edu.cn

© 2016 Chinese Physical Society and IOP Publishing Ltd

2. Experiment

The FZ/FCZ glass samples with the compositions of $53ZrF_4$-$10BaF_2$-$3.9LaF_3$-$3AlF_3$-(10-x)NaF-xNaCl-$10BaCl_2$-$0.1Eu_2O_3$/$53ZrF_4$-$20BaF_2$-(4-y)LaF_3-$3AlF_3$-20NaF-yEu_2O_3 /$53ZrF_4$-$10BaF_2$-$4LaF_3$-(4-y)AlF_3-10NaF-10NaCl-$10BaCl_2$-yEu_2O_3 (values in mol%) named FCZ-xNC ($x = 0$, 2, 4, 6, 8, 10), FZ-2yEu / FCZ-2yEu ($y = 0.01$, 0.1, 0.4, 0.8, 1.2, 1.6, 2.0, 2.4), were prepared by the meltquenching method. The Cl ion percentage concentration of total anions in FCZ-xNC glass is given in Table 1. The raw materials buried in the ammonium fluoride powders were thoroughly mixed in an alumina crucible and then heated at 800 °C for 30 min. The melting product was quickly transferred into a muffle furnace at a temperature of 200 °C under a reducing atmosphere. Followed by cooling to room temperature, the as-prepared transparent samples were presented. The samples were annealed at 260 °C in a reducing atmosphere for 2 h. Finally, cooling to room temperature, the annealed samples were cut and polished into dimensions of approximately $20 \times 20 \times 5$ mm for measurement. The chemicals used in preparation of host glasses were of 99.95% purity in addition to Eu_2O_3 being of 99.99%.

Table 1. Cl ion percentage concentrations of total anions in FCZ-xNC glasses ($x = 0$, 2, 4, 6, 8, 10, 11).

	FCZ-0NC	FCZ-2NC	FCZ-4NC	FCZ-6NC	FCZ-8NC	FCZ-10NC	FCZ-11NC
Cl / (F+Cl)%	6.83	7.51	8.19	8.87	9.56	10.24	10.58

Differential thermal analysis (DTA) was performed using a SHIMADZU DTG-60H with a 10-mg sample under an N_2 atmosphere at a heating rate of 10 °C/min, and the glass sample used for DTA measurements was powdered. The crystal structure of the samples was characterized by using a Rigaku 2500/PC x-ray diffractometer (XRD) with a Cu Ka radiation source (0.1542 nm) at 40 kV and 150 mA. Photoluminescence and time resolved spectrum measurements were performed by a Jobin Yvon FL3 fluorescence spectrophotometer with a 450-W xenon lamp and a flicker frequency 0.05 Hz–25 Hz flashing xenon lamp as an excitation source. All the measurements were carried out in ambient atmosphere.

3. Results and discussion

The DTA curves of FZ/FCZ-6NC/FCZ-10NC/FCZ-11NC samples are given in Fig. 1, the T_g, T_x, T_{p1} are glass transition temperature, initial crystallization temperature, and peak value of crystallization, respectively. The $\Delta T = T_x - T_g$ represents the devitrification tendency, the decreasing value of ΔT signifies the increasing devitrification trends and easier crystallization.[14] These characteristic temperatures are listed in Table 2.

Table 2. DTA parameters of FCZ-xNC glasses ($x = 0$, 6, 10, 11).

	T_g/°C	T_x/°C	T_{p1}/°C	ΔT/°C
FZ	259	341	358	82
FCZ-6NC	258	343	360	85
FCZ-10NC	260	323	342	63
FCZ-11NC	277	378	404	101

The curve of characteristic temperature of the FCZ-6NC sample has little difference from that of FZ glass. Further increasing the concentration of Cl ions, the characteristic temperatures T_x and T_{p1} of FCZ-10NC significantly decrease, and the ΔT also decreases. This result indicates that it is easier for crystallization to happen in the Cl-ions-rich sample. Additionally, the characteristic temperature of the FCZ-11NC sample further confirms this conclusion: the increasing of T_g temperature is due to the partial crystallization of the sample (as shown in Fig. 2) and the melting temperature of crystal is higher than that of the glass phase. The T_g is not changed when it is below a certain critical value, so we choose 260 °C as the annealing temperature, near the glass transition temperature.

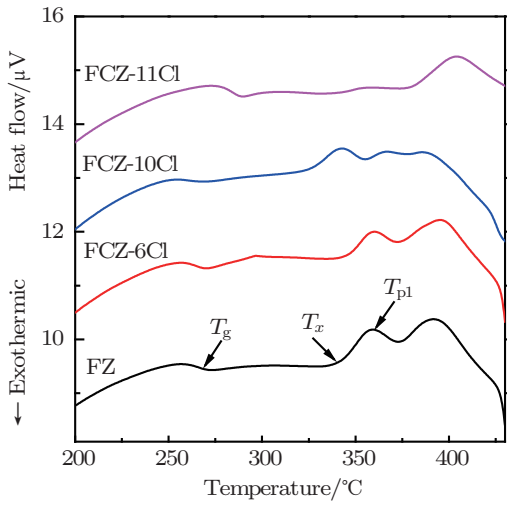


Fig. 1. (color online) Differential thermal analysis (DTA) curves of FCZ-xNC glasses ($x = 0$, 6, 10, 11).

Figure 2 shows the XRD patterns of FZ/FCZ-6NC/FCZ-10NC/FCZ-11NC samples. Except FCZ-11NC, other samples all present two broad typical peaks at about 26° and 47°, indicating that FZ/FCZ-6NC/FCZ-10NC samples are in amorphous glassy states. Most studies have shown that fluorozirconate glass is mainly constitutive ZrF_n polyhedron,[15] because the addition of Cl ions mainly replace F ions connected to the network modifier, and thus will not affect the FZ glass network structure.[12] So the amorphous glassy state still re-

mains in each of these samples. However, several peaks appear on the XRD pattern of the FCZ-11NC sample, which are assigned to mixed phases of $BaZrF_6$ and $BaZr_2F_{10}$ based on the standard XRD pattern. This phenomenon is due to cationic clusters that further cause the separation of the glass phase and the formation of the crystal phase.[15] Meanwhile, these mixed phases lead to increasing the characteristic temperature of the FCZ-11NC sample in the DTA curve.

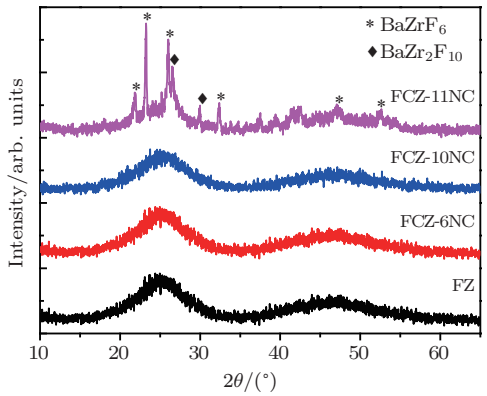


Fig. 2. (color online) XRD patterns of FCZ-*x*NC glasses ($x = 0$, 6, 10, 11).

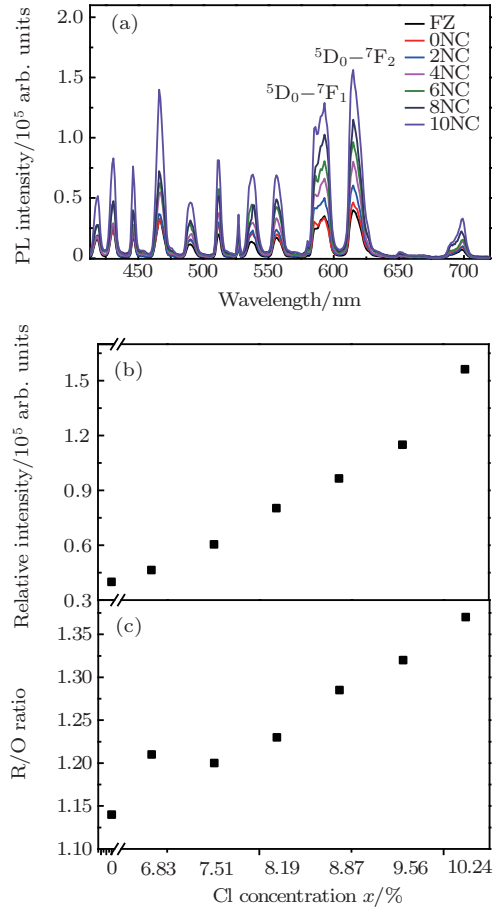


Fig. 3. (color online) (a) PL spectra of FZ/FCZ-*x*NC glasses under 393-nm excitation, (b) luminous intensity analysis of FCZ-*x*NC glasses monitored at 613 nm, (c) R/O ratio of FCZ-*x*NC glasses, where $x = 0$, 2, 4, 6, 8, 10, 11.

Figure 3 shows the photoluminescence (PL) spectra of FZ/FCZ-*x*NC ($x = 0$, 2, 4, 6, 8, and 10) doped with 0.2 mol Eu^{3+} and the variations of luminous intensity of FCZ-*x*NC with Cl ion concentration. Figure 3(a) shows 14 emission bands of Eu^{3+} in all the samples, the most intense emission bands are 613 nm ($^5D_0 \rightarrow {}^7F_1$) and 591 nm ($^5D_0 \rightarrow {}^7F_2$), the next is blue green light emission ($^5D_{3,2,1,0} \rightarrow {}^7F_{4,3,2,1,0}$), radiative transition of $^5D_0 \rightarrow {}^7F_{4,3}$ is relatively weak, luminous intensity of $^5D_0 \rightarrow {}^7F_0$ is the weakest due to forbidding the selection rule. Additionally, the transitions bands of 417 nm–555 nm, which correspond to $^5D_{3,2,1} \rightarrow {}^7F_{4,3,2,1}$ are seldom observed in many glasses,[16–18] which relate to the lower phonon energy in fluorozirconate glass (maximum phonon energy is 590 cm^{-1}).[19] With increasing the concentration of Cl ions, there is no obvious difference in emission location, but the emission intensity is obviously increased, FCZ-10NC is the highest one as shown in Fig. 3(b). The crystalline phase appears in the glass substrate of FCZ-11NC, thus there are no PL spectra of higher concentration samples. The magnetic dipole transition $^5D_0 \rightarrow {}^7F_1$ peaked at 591 nm relates to Eu^{3+} centered at the inversion symmetry in the crystal structure, but the electric dipole transition $^5D_0 \rightarrow {}^7F_2$ with a peak position of 613 nm relates to the Eu^{3+} at non-inversion symmetry. Figure 3(c) shows the curve of the R/O ratio, which is the ratio between intensities of $^5D_0 \rightarrow {}^7F_2$ and $^5D_0 \rightarrow {}^7F_1$ transitions versus Cl ion concentration, the gradually increasing R/O ratio indicates that more Eu^{3+} ions get into the non-inversion symmetry after replacing part of F ions by Cl ions.

In order to further study the influence of Cl ions on the local crystal field environment of Eu^{3+}, we introduce the JO theory to calculate the parameters of the $^5D_0$ level of Eu^{3+} ions in FCZ-*x*NC glasses. The integral strength of emission spectrum and radiation transition probability with JO parameters have the following relationships:[20]

$$\int I_J \mathrm{d}\nu_J \Big/ \int I_{\mathrm{md}} \mathrm{d}\nu_{\mathrm{md}} = \frac{A_J}{A_{\mathrm{md}}}, \tag{1}$$

$$\frac{A_J}{A_{\mathrm{md}}} \propto \Omega_t \langle \varphi' J' \| U^{(J)} \| \varphi J \rangle^2, \tag{2}$$

where I_J, ν_J ($J = 2$, 4) are the electric dipole transition peak area and the corresponding wave numbers, I_{md} and ν_{md} are the magnetic dipole transition peak area and the corresponding wave numbers, A_J and A_{md} are the electric dipole transition probability and the magnetic dipole transition probability, Ω_t ($t = 2$, 4) are the JO parameters, and $\langle \varphi' J' \| U^{(J)} \| \varphi J \rangle^2$ is the emission-reduced matrix elements. The electronic transition occurs from initial state J to final state J'. The calculation results are listed in Table 3. The JO parameter Ω_2 relates to the ligand field symmetry of the rare earth ions within the glass: the larger the value of Ω_2, the lower the symmetry will be; on the contrary, the smaller the value of Ω_2, the higher the symmetry will be.[21] It is noted that Ω_2 increases with the increasing Cl ion concentration, which results in the decrease of the Eu^{3+} local symmetry. Both the Cl and F ions appearing in the first coordination shell of Eu^{3+} change the symmetry.[22]

Table 3. Values of JO parameters Ω_2/Ω_4, calculated lifetime τ_{tal}, experimental lifetime τ_{exp}, fitting lifetimes τ_1 and τ_2, fluorescence branching ratios A_1 and A_2, quantum efficiency η of Eu^{3+} $^5D_0$ energy level for FCZ-xNC glasses ($x = 0, 2, 4, 6, 8, 10$).

	FCZ-0NC	FCZ-2NC	FCZ-4NC	FCZ-6NC	FCZ-8NC	FCZ-10NC
$\Omega_2/10^{-20}$ cm^2	2.98	3.12	3.35	3.64	3.82	3.96
$\Omega_4/10^{-20}$ cm^2	2.46	2.36	2.09	2.15	2.42	2.52
τ_1/ms	1.70	1.69	1.66	1.66	1.65	1.61
τ_2/ms	5.03	5.06	5.13	5.14	5.17	5.23
A_1/%	17.7	17.1	15.8	13.3	11.1	7.9
A_2/%	82.3	82.9	84.2	86.7	88.9	92.1
τ_{tal}/ms	7.16	7.18	7.20	7.22	7.23	7.27
τ_{exp}/ms	4.80	4.84	4.93	4.97	5.03	5.14
η/%	67.0	67.4	68.5	68.8	69.6	70.7

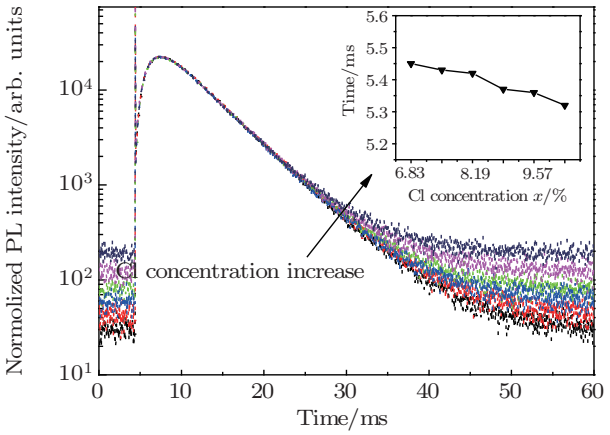


Fig. 4. (color online) Normolized fluorescence decay curves of FCZ-xNC glasses at room-temperature of the $^5D_0 \rightarrow {}^7F_2$ transition excited at 393 nm, monitored at 613 nm. Inset: double-exponential fitted lifetime of FCZ-xNC glasses, where $x = 0, 2, 4, 6, 8, 10, 11$.

Figure 4 shows the normalized fluorescence intensity decay curves of FCZ-xNC glasses. All the curves increase with time obviously initially. The risetime can be explained by the excited-state absorption of higher levels ($^5D_1$) or energy transfer from neighboring Eu^{3+} ions.[19] All curves fit to double-exponential decay, the average lifetime of Eu^{3+} ions can be expressed as

$$\tau_{exp} = \left(A_1\tau_1^2 + A_2\tau_2^2\right)/(A_1\tau_1 + A_2\tau_2), \quad (3)$$

where τ_1 and τ_2 represent short-lifetime and long-lifetime, A_1 and A_2 are the fluorescence branching ratios corresponding to the τ_1 and τ_2. The fitting results are shown in Table 3. The results imply that there are two kinds of sites for Eu^{3+} ions in a glass network due to different lifetimes τ_1 and τ_2.[19] The lifetimes τ_1 and τ_2 are corresponding to the different sites of Eu^{3+} ions: τ_2 is larger than τ_1. With Cl concentration increasing, the average lifetime τ_{exp} increases while τ_1 and A_1 decrease, which is contrary to the scenario of τ_2 and A_2. This result shows that the number of Eu^{3+} ions at the site decreases with lifetime τ_1 increasing and that at the other site increases with τ_2 increasing. The estimated quantum efficiency τ_{exp}/τ_{cal} increases from 62.4% to 80.2%, the calculated lifetimes τ_{cal} from JO theory are also listed in Table 3.

Figure 5 shows the luminous intensity point diagram of different concentrations of Eu^{3+} in FZ-2yEu and FCZ-2yEu glass samples. Under the same concentration of Eu^{3+}, luminous intensities of all the glasses containing the Cl ion increase. We find that the Cl ion causes no change of the best Eu^{3+} doping concentration (peaked at 3.2 mol) in FZ glass, which demonstrates that the introduction of Cl ion does not affect the Eu^{3+} solubility in the glass matrix.

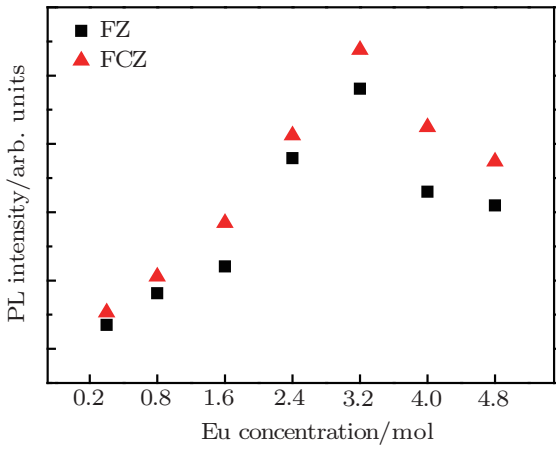


Fig. 5. (color online) Variations of luminous intensity of $^5D_0 \rightarrow {}^7F_2$ transition in FZ and FCZ-10NC glasses with the concentration of Eu^{3+} ions excited at 393 nm.

Figures 6(a) and 6(b) show the time-dependent normalized fluorescence decay curves of FZ-2yEu and FCZ-2yEu glasses for different concentrations of Eu^{3+} ions, respectively. Fitting results indicate that fluorescence decays of FCZ glass are slightly higher than that of FZ glass under the same concentration of Eu^{3+} ions as shown in Fig. 6(c). With increasing the concentration of Eu^{3+} ions, the average lifetime τ_{exp} (hollow) first increases then decreases. This change of lifetime is consistent with that of luminous intensity. The lifetime decreases when the Eu^{3+} concentration is over 3.2 mol due to the self-quenching. The best doping concentration corresponds to the longest lifetime. The introduction of Cl ions does not affect the variation trend of lifetime. The lifetime τ_{cal} (solid) calculated from JO theory is given at the same time, and the theoretical simulation is in accordance with the experimental result. Figure 6(d) gives the estimated quantum efficiency, showing that the quantum efficiency is increased by 3∼4% in all FCZ-2yEu glasses due to the introduction of Cl ions.

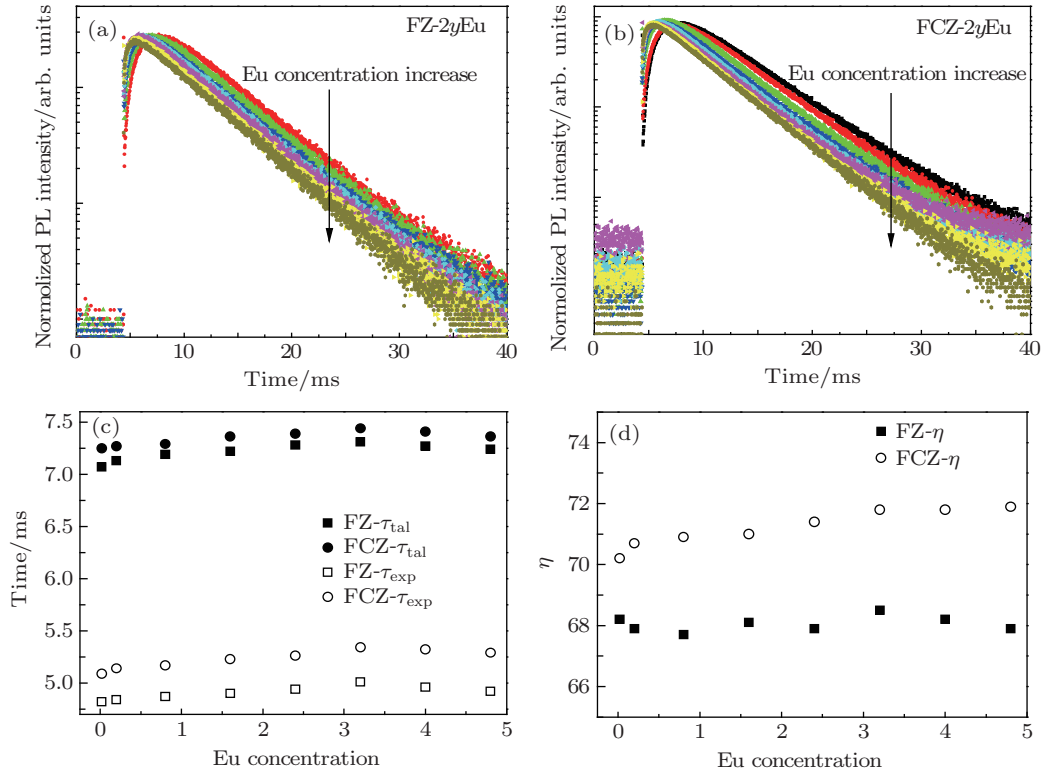


Fig. 6. (color online) (a) normolized fluorescence decay curves of FZ-2*y*Eu ($y = 0.02$–4.8 mol) glasses, (b) normolized fluorescence decay curves of FCZ-2*y*Eu ($y = 0.02$–4.8 mol) glasses excited at 393 nm, monitored at 613 nm, (c) calculated lifetime τ_{tal} (solid), and experimental lifetime τ_{exp} (empty) values for FZ-2*y*Eu and FCZ-2*y*Eu glasses, (d) quantum efficiency η values of FZ-2*y*Eu and FCZ-2*y*Eu glasses respectively.

4. Conclusions

A series of Eu^{3+} ions doped fluorozirconate glasses containing chloride ions are prepared. The introduction of Cl ions reduces the glass crystallization temperature, and increases the devitrification trend of fluorozirconate glass, leading to the crystalline phase forming more easily. Cationic clusters lead to the separation of the glass phase and the generation of the $BaZrF_6/BaZr_2F_{10}$ phase, when the Cl ion concentration exceeds 10.24%. The luminous intensity of Eu^{3+} ions is dramatically enhanced with the increase of Cl ion concentration, and the quantum efficiency is increased from 67.0% to 70.7% at the same time. The doped Cl ions can reduce the local symmetry of Eu^{3+} ions, indicated by analyzing the R/O ratio and JO parameters. Fluorescence decay analysis reveals that there are two kinds of sites for Eu^{3+} ions in a glass network, corresponding to short-lifetime and long-lifetime, respectively. The average lifetime increases with increasing the concentration of Cl ions. Moreover, the proportion of Eu^{3+} with a long-lifetime is improved, while that with the short-lifetime is opposite. Additionally, the substitution of the Cl ion for the F ion does not affect the solubility of rare earth Eu^{3+} ion nor the variation trend of fluorescence decay under different Eu^{3+} concentrations, and the best doping concentration corresponds to the longest fluorescence decay. In a word, the introduction of the Cl ions can strengthen the luminous intensity of glass, increase the average lifetime and improve quantum efficiency by about 3%–4%.

References

[1] Sun J, Zhang X S, Yuan L L, Feng Z J, Ling Z and Li L 2014 *Chin. Phys. B* **23** 114103
[2] Wang T S, Duan B H, Tian F, Peng H B, Chen L, Zhang L M and Yuan W 2015 *Chin. Phys. B* **24** 076102
[3] Li Q Y, Xu X H, Zhang B H, Wu Y M, Qiu J B and Yu X 2014 *Chin. Phys. B* **23** 127803
[4] Merigeon J, Maalej O, Boulard B, Stanculescu A, Leontie L, Mardare D and Girtan M 2015 *Opt. Mater.* **48** 243
[5] Lachheb R, Damak K, Assadi A A, Herrmann A, Yousef E, Rüssel C and Maâlej R 2015 *J. Lumin.* **161** 281
[6] Pfau C, Bohley C, Miclea P T and Schweizer S 2011 *J. Appl. Phycol.* **109** 083545
[7] Bendow B, Banerjee P K, Drexhage M G, Goltman J, Mitra S S and Moynihan C T 1982 *J. Am. Chem. Soc.* **65** C8
[8] Bendow B, Drexhage M G and Lipson H G 1981 *J. Appl. Phys.* **52** 1460
[9] Inoue S, Soga K and Makishima A 1993 *J. Am. Chem. Soc.* **76** 1591
[10] Ahrens B, Brand S, Büchner T, Darr P, Schoenfelder S, Paßlick C and Schweizer S 2011 *J. Non-Cryst. Solids* **357** 2264
[11] Poulain M 1983 *J. Non-Cryst. Solids* **56** 1
[12] Soga K, Inoue H and Makishima A 2000 *J. Non-Cryst. Solids* **274** 69
[13] Edgar A, Schweizer S, Assmann S, Spaeth J M, Newman P J and MacFarlane D R 2001 *J. Non-Cryst. Solids* **284** 237
[14] Yu C, Zhang J, Wang G and Jiang Z H 2008 *J. Alloys Compd.* **461** 378
[15] Hendy S C and Edgar A 2006 *J. Non-Cryst. Solids* **352** 415
[16] Rajesh D, Brahmachary K, Ratnakaram Y C, Kiran N, Baker A P and Wang G G 2015 *J. Alloys Compd.* **646** 1096
[17] Fan S, Yu C, He D, Li K and Hu L 2012 *J. Alloys Compd.* **518** 80
[18] Pisarski W A, Zur L, Kowal M and Pisarska J 2015 *J. Alloys Compd.* **651** 565
[19] Maalej O, EI Jouad M, Gaumer N, Chaussedent S, Boulard B and Dammak Ben Ameur M, Dammak Ben Tijani D 2015 *J. Non-Cryst. Solids* **420** 48
[20] Kalpana T, Brik M G, Sudarsan V, Naresh P, Ravi Kumar V, Kityk I V and Veeraiah N 2015 *J. Non-Cryst. Solids* **419** 75
[21] Tian Y, Xu R, Hu L and Zhang J 2012 *J. Lumin.* **132** 128
[22] Soga K and Inoue H and Makishima A 1993 *J. Lumin.* **55** 17